metals

MDPI

Article

Electrochemical Corrosion Behavior of Passivated Precipitation Hardening Stainless Steels for Aerospace Applications

José Villegas-Tovar [1], Citlalli Gaona-Tiburcio [1], María Lara-Banda [1], Erick Maldonado-Bandala [2,*], Miguel Angel Baltazar-Zamora [2], Jose Cabral-Miramontes [1], Demetrio Nieves-Mendoza [2], Javier Olguin-Coca [3], Francisco Estupiñan-Lopez [1] and Facundo Almeraya-Calderón [1,*]

[1] Centro de Investigación e Innovación en Ingeniería Aeronáutica (CIIIA), Universidad Autónoma de Nuevo León, FIME, San Nicolás de los Garza 66455, Mexico; miguel.villegastvr@uanl.edu.mx (J.V.-T.); citlalli.gaonatbr@uanl.edu.mx (C.G.-T.); maria.laraba@uanl.edu.mx (M.L.-B.); jose.cabralmr@uanl.edu.mx (J.C.-M.); francisco.estupinanlp@uanl.edu.mx (F.E.-L.)
[2] Facultad de Ingeniería Civil, Universidad Veracruzana, Xalapa 91000, Mexico; dnieves@uv.mx (D.N.-M.)
[3] Área Académica de Ingeniería y Arquitectura, Universidad Autónoma del Estado de Hidalgo, Carretera Pachuca-Tulancingo Km. 4.5. Hidalgo, Pachuca 42082, Mexico; olguinc@uaeh.edu.mx
* Correspondence: erimaldonado@uv.mx (E.M.-B.); facundo.almerayacld@uanl.edu.mx (F.A.-C.)

Abstract: Precipitation-hardening (PH) stainless steels (SS) are widely used in various aerospace applications. These steels exhibit good mechanical and corrosion resistance. The electrochemical behavior of 15-5PH, 17-4PH, Custom450 and AM 350 stainless steels passivated with citric and nitric acid baths for 60 and 90 min at 25 and 49 °C were evaluated in 5 wt.% sodium chloride (NaCl) and 1 wt.% sulfuric acid (H_2SO_4) solutions. The electrochemical behavior was studied with potentiodynamic polarization curves (PPC) according to the ASTM G5-13 standard. The results indicated that there are two characteristic mechanisms that are present in the potentiodynamic polarization curves. When the PHSS is immersed in an H_2SO_4 solution, there is a secondary passivation, and in the NaCl solution, there is a pseudo-passivation (not stable passivation film). The current densities in the NaCl solution were between 10^{-4} and 10^{-5} mA/cm^2, while those of H_2SO_4 were recorded around 10^{-2} and 10^{-3} mA/cm^2. Citric acid does work as a passivating solution, and in some cases, the corrosion resistance of the stainless steel was comparable to that of nitric acid.

Keywords: corrosion; potentiodynamic polarization; precipitation hardening; stainless steels

Citation: Villegas-Tovar, J.; Gaona-Tiburcio, C.; Lara-Banda, M.; Maldonado-Bandala, E.; Baltazar-Zamora, M.A.; Cabral-Miramontes, J.; Nieves-Mendoza, D.; Olguin-Coca, J.; Estupiñan-Lopez, F.; Almeraya-Calderón, F. Electrochemical Corrosion Behavior of Passivated Precipitation Hardening Stainless Steels for Aerospace Applications. *Metals* **2023**, *13*, 835. https://doi.org/10.3390/met13050835

Academic Editor: Eric Hug

Received: 10 April 2023
Revised: 17 April 2023
Accepted: 20 April 2023
Published: 24 April 2023

1. Introduction

Environmental regulations in the aeronautical industry suggest using ecological and environmentally sustainable corrosion protection treatments. The chemical treatment known as passivation is a typical coating on stainless steel that helps improve its resistance to corrosion [1–3].

Iron-based alloys containing at least 11% chromium are known as stainless steels. With chromium content and other elements, stainless steel can provide an extraordinary range of corrosion resistance. The SS are classified into five distinct families according to their crystalline structure and precipitates [1,4].

The use of precipitation-hardening stainless steels (PHSS) in the aerospace industry is low, but they are essential for some components. It is a family that can be used for its excellent properties (low weight and high mechanical and corrosion resistance) [3,5]. PHSS can be semi-austenitic and martensitic. The semi-austenitic type is essentially austenitic stainless steel with annealing heat treatment, which is then heat treated where the austenitic phase transforms into the martensitic phase for subsequent precipitation hardening. Martensitic types are already stainless steel in the solution annealed condition and only require precipitation hardening after manufacturing [6–10].

The most widely used PHSS in the aerospace industry are 15-5PH, 17-4PH, Custom450 (martensitic) and AM350 (semi-austenitic) [8]. The most important applications of these PHSS are in the manufacture of turbine blades for Custom450, while AM350 is used for shafts, rotors, and turbine blades. Finally, 15-5PH and 17-4PH are used in structural components such as flaps [11–13].

Stainless steels have good corrosion resistance because they naturally form a thin and invisible surface oxide film. This film is an oxide that protects the steel from chemical attack in an aggressive environment, thus preventing corrosion. The passivation process is a surface treatment that allows the steel to improve its resistance to corrosion, having a more resistant chromium oxide film that forms. Naturally, this film is continuous, adherent, and compact [8,14]. To obtain a chromium oxide film, it is necessary that the steel contain at least 11% chromium: the passivity increases as the chromium content is higher in the steel. For this reason, many stainless steels contain 17–18% chromium as an alloying element. The passive film is self-healing, unlike other coatings such as paints [13–15].

In the aeronautical industry, the corrosion costs are high, in addition to aircraft downtime, environmental risks, and possible human losses [8]. In the passivation process, nitric acid (HNO_3) is a strong oxidant and promotes the formation of passive films on stainless steels [15]. In recent years, citric acid ($C_6H_8O_7$) has become a sustainable alternative passivating agent for HNO_3 since it is not toxic and is friendly to the environment. This acid can be extracted from fruits and vegetables and is also low-cost. $C_6H_8O_7$ is generally applied in a solution of around 10%, while the HNO_3 can reach solutions up to 40%. Both solutions are used for the same time and temperature, although the HNO_3 is used in a lower temperature range [16,17].

Electrochemical techniques used in corrosion studies are an important tool for understanding the behavior of metallic materials. Potentiodynamic polarization is a technique where the potential of an electrode (stainless steel) is polarized to determine the corrosion rate. One of the most widely used methods to calculate the corrosion rate is the Tafel extrapolation method, where it can be appreciated that both the anodic branch (upper) and the cathodic branch (lower) present a linearity between 50 to 100 mV [18,19].

El-Taib Heakal et al. [20] studied the corrosion behavior of austenitic stainless steels in aerated and deaerated solutions. The electrochemical characterization was carried out by using potentiodynamic polarization and electrochemical impedance spectroscopy, and the results indicated that the pH decreases with the current density due to the alloying elements. In another study, El-Taib Heakal et al. [21] evaluated stainless steels containing molybdenum in order to investigate the behavior of the natural growth of the passive film. Ameer et al. [22] reported i_{corr} values that increased with increasing either Cl^- or SO_4^{2-} concentration, characterized by potentiodynamic polarization in stainless steel. This represents a decrease in the formation of the passive film. The evaluation of passivated 304, 15-5PH, and 17-4PH stainless steel employing electrochemical noise and potentiodynamic polarization indicated that a similar passive layer was formed [23]. Bragaglia et al. [24] used PP to observe the behavior of passivated and unpassivated 304 austenitic stainless steel in acid electrolytes. The pitting potential in nitric acid increases when the steel is passivated. Marcelin et al. [25] studied the corrosion behavior of martensitic stainless steel. The results showed that the electrochemical process was controlled by passive film properties. Recent investigations on precipitation-hardening stainless steels have focused on fatigue behavior, hydrogen diffusion, and microstructural characterization [13,26–28]. Gaona et al. [29] studied the corrosion behavior of AM350 passivated PHSS steels using electrochemical noise, potentiodynamic polarization and electrochemical impedance spectroscopy in acid baths. The martensitic precipitation hardening stainless steels showed the best results for corrosion behavior in acid solutions.

Over the past few years, the corrosion behavior of austenitic stainless steels has been extensively studied. There are few studies on passivated PHSS, so it is important to know the behavior of electrochemical corrosion in environments that simulate aircraft working conditions, such as marine and industrial atmospheres.

The present work aims to study the electrochemical behavior of PHSS (15-5PH, 17-4PH, Custom450, and AM350) from the Potentiodynamic Polarization (PP) using $C_6H_8O_7$ and HNO_3 as passivating agents, having as variables the passivation temperature and immersion time, exposed to NaCl and H_2SO_4 solutions.

2. Materials and Methods

2.1. Materials

The employed stainless steels (AMS Aerospace Material Specifications) were 15-5PH (AMS 5659), 17-4PH (AMS 5643), Custom 450 (AMS 5773), and AM 350 (AMS 5548) in cylindrical bar form. The nominal chemical composition of these PHSS is shown in Table 1.

Table 1. The chemical composition of the used stainless steel (wt.%) [30–33].

PHSS	Elements											
	Cr	Ni	Mo	Mn	Cu	Ti	Nb	N	Si	S	C	Fe
15-5PH	14.0–15.5	3.5–5.5	–	1.0 max.	2.5–4.5	–	0.15–0.45	–	1.0 max.	0.03 max.	0.07 max	Balance
17-4PH	15.0–17.5	3.0–5.0	0.50	1.0 max.	3.0–5.0	–	0.15–0.45	–	–	0.03 max.	0.07 max.	Balance
Custom 450	14.0–16.0	5.0–7.0	0.50–1.0	1.00	1.25–1.75	0.90–1.40	0.5–0.75	≤0.1	1.00	0.030	≤0.05	Balance
AM350	16.0–17.0	4.0–5.0	2.50–3.25	0.50–1.25	–	–	–	0.07–0.13	≤0.50	0.030	0.07–0.11	Balance

From the cylindrical steel bar, coupons of approximately 0.5 cm thickness were obtained according to ASTM A380/A380M [34]. Each sample was roughed with silicon carbide abrasive paper up to #600 [35]. In this way, the working electrode (anode) was obtained, which was washed in an acetone solution in ultrasound to obtain a homogeneous surface without contaminants. Optical microscopy (OM, Olympus, Hamburg, Germany) was used to determine the microstructure of PHSS.

2.2. Passivation Treatment

The passivation treatment was performed according to ASTM G967 and SAE/ASM2700 standards [17,36]. The following were control variables: passivation solution, passivation temperature, and passivation time (see Figure 1).

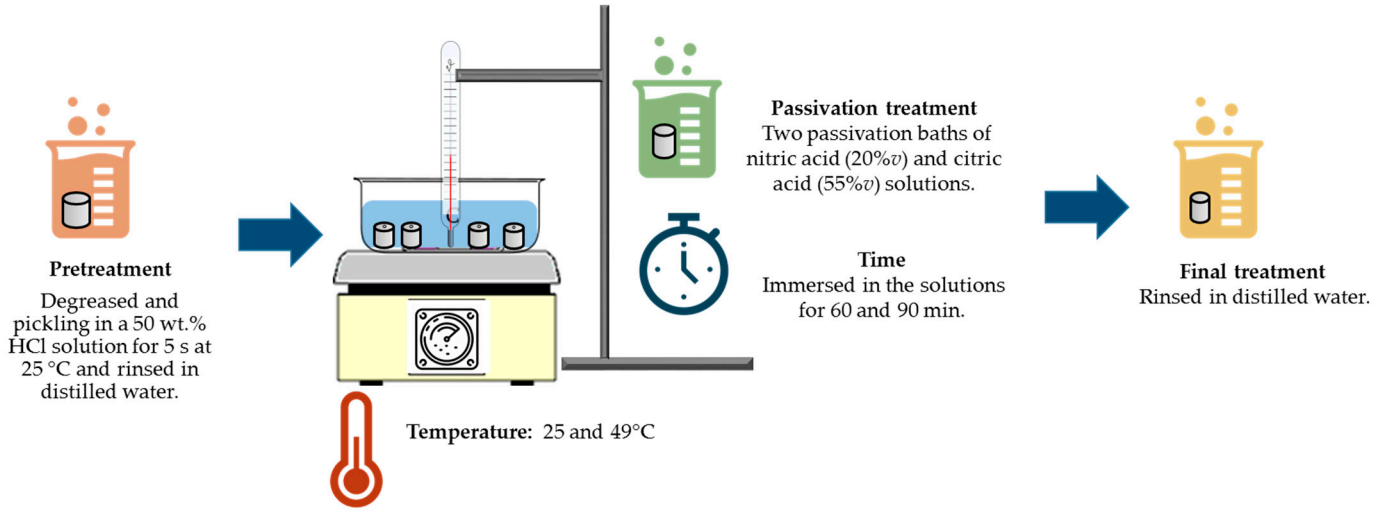

Figure 1. Diagram of passivation treatment of PHSS in citric and nitric acid baths.

The passivation treatment consisted of the following steps:

(a) Pretreatment: degreased and pickled stainless steel in a 50 wt.% HCl solution (analytical grade reagents (J.T. Baker, Nuevo León, México) for 5 s at 25 °C, and rinsed in distilled water.

(b) Passivation: two passivation bath solutions were used [citric acid (55%v) and nitric acid (20%v), the rest is distilled water (analytical grade reagents (J.T. Baker))]. A constant temperature of 25 and 49 °C. Samples were immersed in the solutions for 60 and 90 min [28,29].

(c) Final Stage: the specimens were rinsed in distilled water (analytical grade reagents (J.T. Baker)).

All these processes were completed for each passivating solution and for each material. According to the experimental matrix, a total of 32 experiments were performed.

2.3. Corrosion Tests

Corrosion tests were performed at room temperature using Gill AC equipment (potentiostat/galvanostat), evaluated in 5 wt.% sodium chloride (NaCl) and 1 wt.% sulfuric acid (H_2SO_4) solutions. A typical corrosion cell with three electrodes was used: a working electrode, WE (passivated stainless steel), a reference electrode (saturated calomel (SCE)), and a counter electrode (CE), a platinum mesh (Figure 2). The following parameters were used for the electrochemical technique of potentiodynamic polarization (PP): a potential range was used between −1.0 and 1.2 V of OCP, and a sweep rate of 0.06 V/min was applied, according to ASTM G5-11 [37–40].

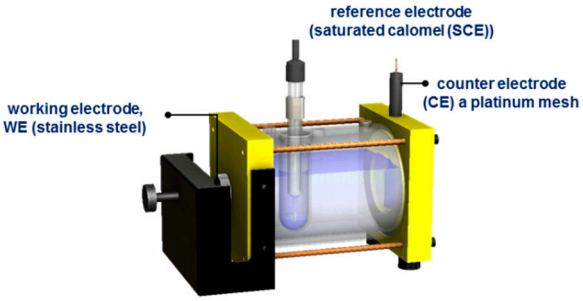

Figure 2. Conventional three-electrode corrosion cell.

Figure 3 shows the flow diagram of the experimentation of the Electrochemical Corrosion Behavior of Passivated Precipitation Hardening Stainless Steels.

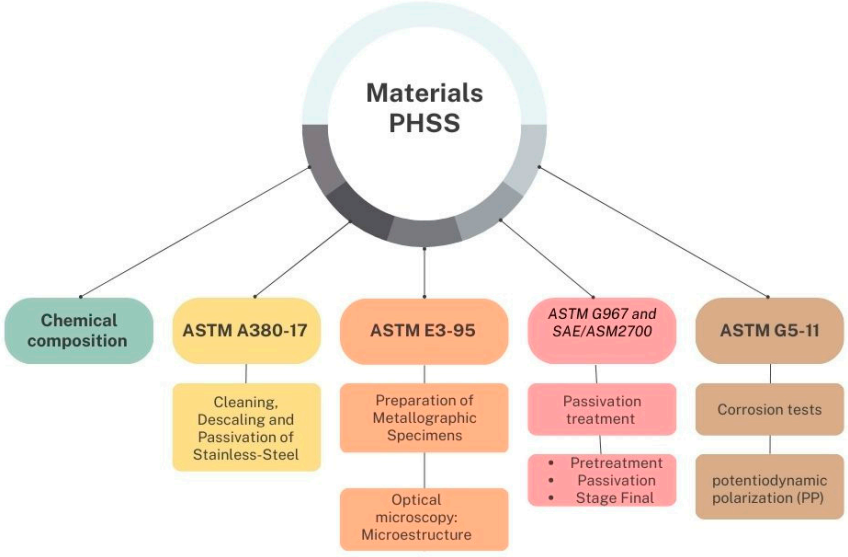

Figure 3. Experimentation flow diagram.

3. Results and Discussion

3.1. OM Microstructural Analysis

The microstructure of the steels under study was obtained by optical microscopy. In Figure 4, the martensitic steel (17-4PH, 15-5PH, and Custom 450) showed a martensitic (α') phase, while the AM350 semi-austenitic stainless steel presented a microstructure of delta (δ) ferrite phase and austenite (γ) [41–43].

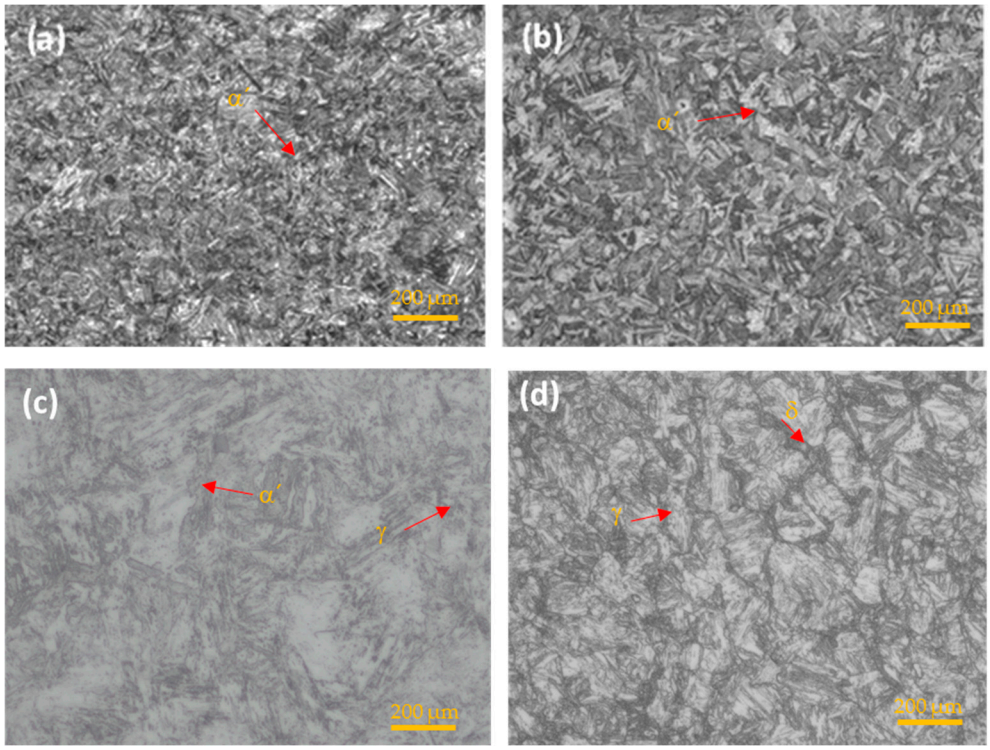

Figure 4. OM microstructure of PHSS. (**a**) 15-5PH, (**b**) 17-4PH, (**c**) Custom 450, and (**d**) AM 350.

In stainless steel, the carbon content decreases corrosion resistance. Still, it increases toughness and causes greater susceptibility to the formation of chromium carbides that can embrittle the material due to precipitation at grain boundaries.

Resistance to pitting corrosion can be measured using the pitting resistance equivalent number (PREN). This parameter is based on the chemical composition of stainless steels, and the PREN result indicated greater resistance to pitting corrosion at high values [44–46]: see Table 2. It is calculated (Equation (1)) based on the chromium (Cr), molybdenum (Mo), tungsten (W), and nitrogen (N) content of an alloy [47]. In this sense, of the four materials evaluated in this work, the AM350 and 15-5PH materials were the ones that presented the highest PREN values of 29.80 and 23.5, respectively, while the Custom 450 and 17-4PH materials presented lower values. Therefore, based on these results, PHSS AM350 and 15-5PH should present greater resistance to pitting corrosion (See Table 2).

$$\text{PREN} = \text{Cr} + 3.3\text{Mo} + 16\text{N} \quad (1)$$

3.2. Potentiodynamic Polarization

The corrosion kinetic behavior using potentiodynamic polarization can be observed through cathodic and anodic reactions in polarization curves to obtain the electrochemical parameters (corrosion current density, i_{corr} ($\mu A \cdot cm^2$), potential corrosion, E_{corr} (mV), and corrosion rate). The Tafel extrapolation technique is used [48–50]. Figures 5 and 6 show the PP curves obtained for PHSS passivated in acid baths at 25 and 49 °C for 60 and 90 min and immersed in 5 wt.% NaCl and 1 wt.% H_2SO_4 solutions.

Table 2. Pitting resistance equivalent numbers of the martensitic and semi-austenitic precipitation hardening stainless steel.

PHSS	Cr	Mo	N	PREN
15-5PH	14.0–15.5	–	0.50	23.5
17-4PH	15.0–17.5	–	–	17.5
Custom 450	14.0–16.0	0.50–1.0	≤0.1	20.9
AM350	16.0–17.0	2.50–3.25	0.07–0.13	29.80

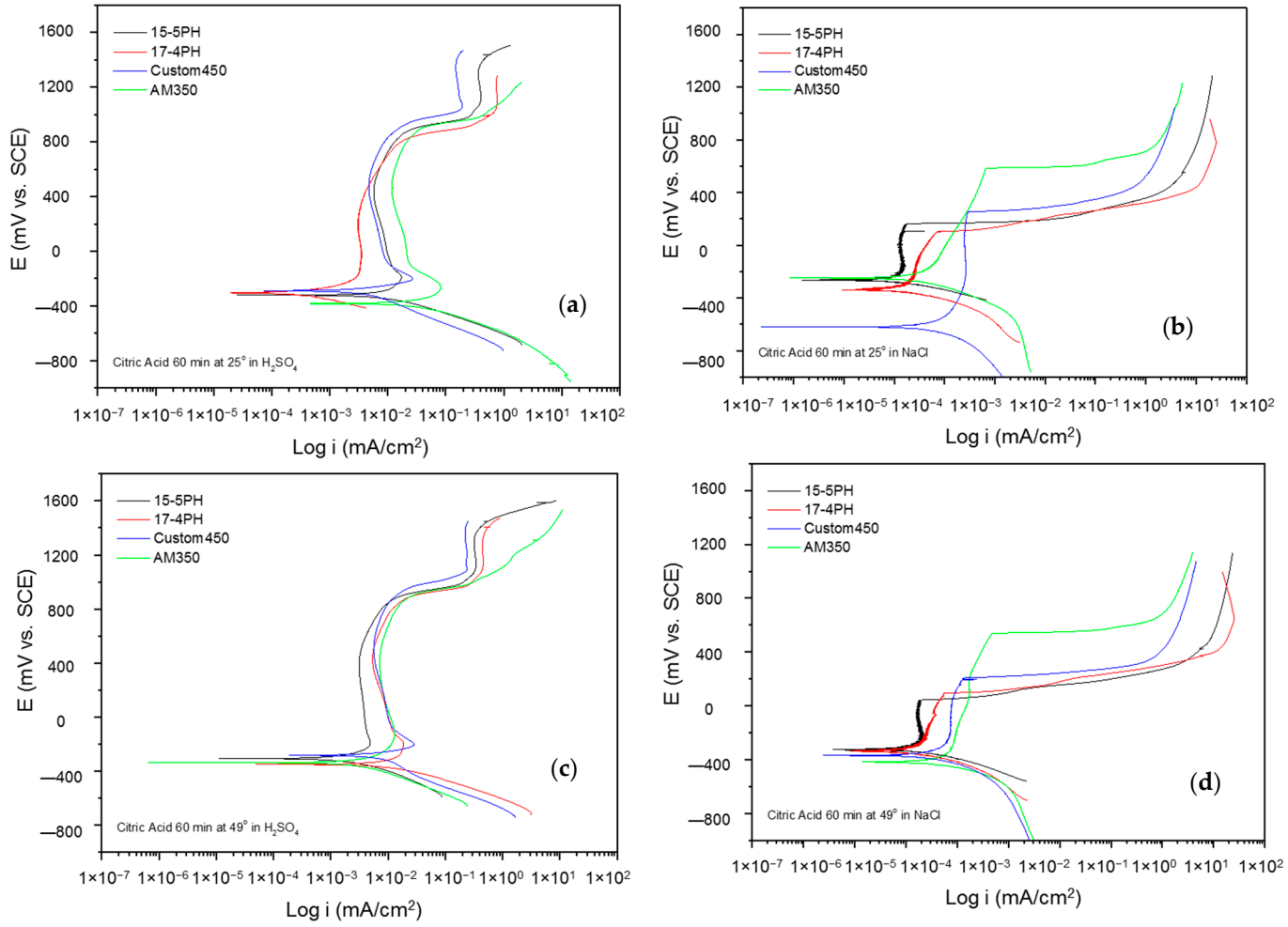

Figure 5. Potentiodynamic polarization curves for passivated PHSS in citric acid, at 25 and 49 °C for 60 min: (**a**,**c**) H_2SO_4 and (**b**,**d**) NaCl solutions.

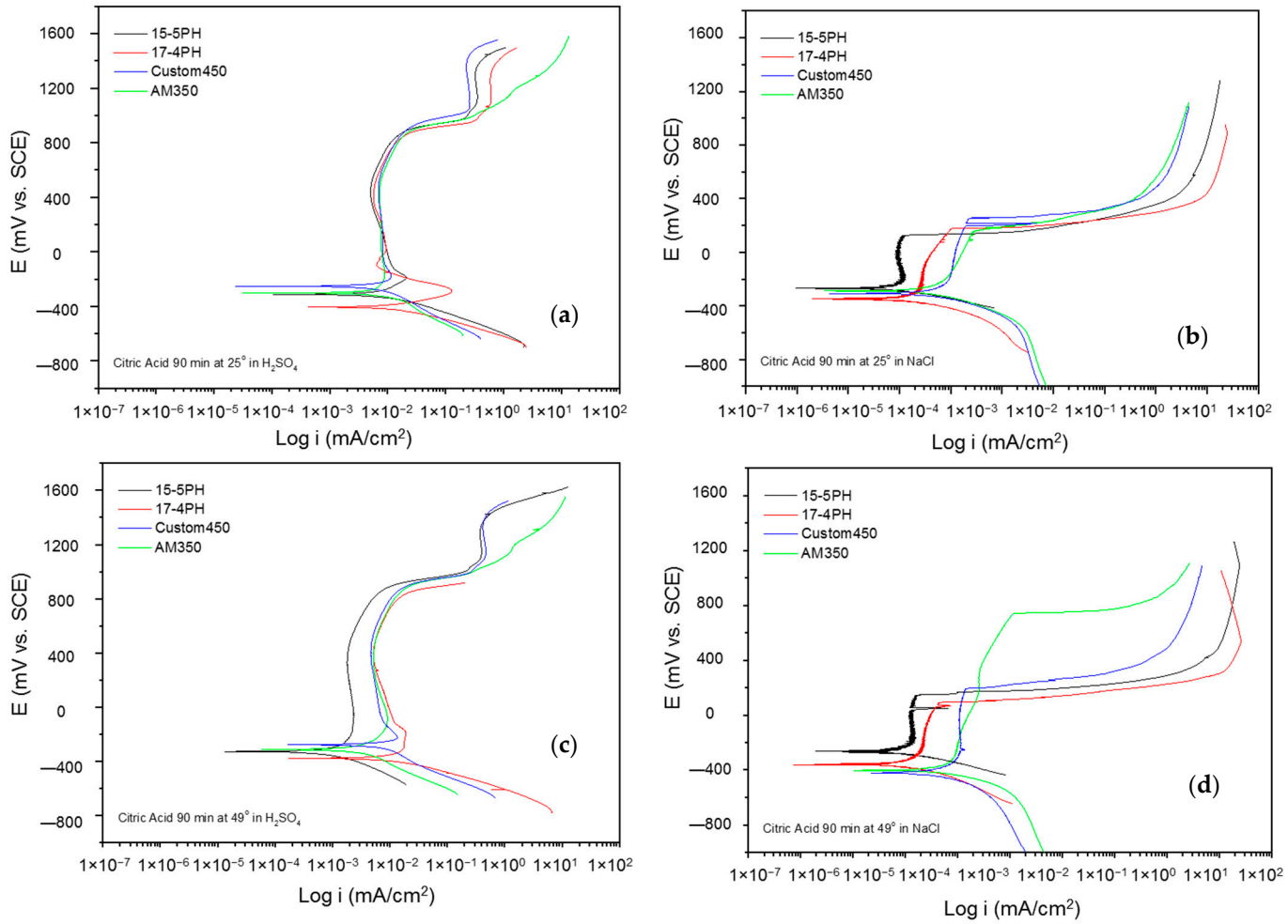

Figure 6. Potentiodynamic polarization curves for passivated PHSS in citric acid, at 25 and 49 °C for 90 min: (**a**,**c**) H_2SO_4 and (**b**,**d**) NaCl solutions.

In general, the PPC represents the corrosion potential vs. the logarithm of the current, indicating a mixed control by activation which, in turn, reveals the behavior of the corrosion kinetics. The parameters obtained from potentiodynamic polarization (PP) curves are summarized in Tables 3–6.

Table 3. Electrochemical parameters obtained by PPC for passivated PHSS in citric acid at 60 min exposed to H_2SO_4 and NaCl solutions.

Solution	PHSS	Temp. (°C)	E_{corr} (mV)	E_{pit} (mV)	i_{corr} (mA/cm^2)	i_{pass} (mA/cm^2)	Range Passive (mV)	Corrosion Rate (mm/y)
H_2SO_4	15-5PH	25	−326	862	3.96×10^{-3}	7.73×10^{-3}	632	8.13×10^{-5}
		49	−305	837	2.17×10^{-3}	3.51×10^{-3}	616	1.55×10^{-5}
	17-4PH	25	−332	789	1.44×10^{-3}	3.18×10^{-3}	394	3.93×10^{-6}
		49	−353	863	1.52×10^{-2}	7.61×10^{-3}	640	6.58×10^{-5}
	Custom 450	25	−312	768	9.52×10^{-3}	5.64×10^{-3}	722	8.68×10^{-3}
		49	−279	916	1.13×10^{-2}	7.69×10^{-3}	778	1.45×10^{-2}
	AM350	25	−247	586	4.64×10^{-4}	1.53×10^{-2}	737	1.06×10^{-2}
		49	−337	840	5.35×10^{-3}	7.31×10^{-3}	680	7.16×10^{-3}

Table 3. *Cont.*

Solution	PHSS	Temp. (°C)	E_{corr} (mV)	E_{pit} (mV)	i_{corr} (mA/cm^2)	i_{pass} (mA/cm^2)	Range Passive (mV)	Corrosion Rate (mm/y)
NaCl	15-5PH	25	−263	161	1.03×10^{-4}	1.41×10^{-4}	329	5.22×10^{-7}
		49	−322	45	1.29×10^{-4}	1.76×10^{-4}	267	5.54×10^{-7}
	17-4PH	25	−340	105	1.63×10^{-4}	2.37×10^{-4} *	335 *	7.91×10^{-7}
		49	−334	95	1.51×10^{-4}	2.52×10^{-4} *	338 *	9.64×10^{-7}
	Custom 450	25	−619	251	8.29×10^{-4}	2.59×10^{-3}	518	7.57×10^{-4}
		49	−369	203	3.68×10^{-4}	7.42×10^{-4}	304	3.91×10^{-4}
	AM350	25	−249	586	2.96×10^{-4}	6.83×10^{-4} *	711 *	8.52×10^{-5}
		49	−417	539	4.12×10^{-4}	8.08×10^{-4} *	849 *	9.01×10^{-4}

* pseudo-passivation.

Table 4. Electrochemical parameters obtained by PPC for passivated PHSS in nitric acid at 60 min exposed to H_2SO_4 and NaCl solutions.

Solution	PHSS	Temp. (°C)	E_{corr} (mV)	E_{pit} (mV)	i_{corr} (mA/cm^2)	i_{pass} (mA/cm^2)	Range Passive (mV)	Corrosion Rate (mm/y)
H_2SO_4	15-5PH	25	−329	831	1.30×10^{-3}	3.17×10^{-3}	731	3.67×10^{-6}
		49	46	601	3.87×10^{-5}	1.34×10^{-4}	657	1.01×10^{-6}
	17-4PH	25	−296	815	1.39×10^{-2}	3.12×10^{-3}	508	1.17×10^{-5}
		49	−352	819	2.85×10^{-3}	3.09×10^{-4}	530	4.47×10^{-7}
	Custom 450	25	−279	936	2.97×10^{-3}	5.14×10^{-3}	711	1.52×10^{-2}
		49	−241	937	5.36×10^{-3}	1.47×10^{-3}	878	6.41×10^{-3}
	AM350	25	−288	874	1.22×10^{-3}	3.92×10^{-3}	575	4.74×10^{-3}
		49	−360	882	4.78×10^{-3}	1.43×10^{-2}	994	5.11×10^{-2}
NaCl	15-5PH	25	−291	116	4.53×10^{-5}	6.42×10^{-5}	212	3.63×10^{-7}
		49	−239	425	4.34×10^{-5}	6.16×10^{-5}	251	2.28×10^{-7}
	17-4PH	25	−200	275	8.75×10^{-5}	1.24×10^{-4} *	394 *	5.66×10^{-7}
		49	−275	400	6.43×10^{-5}	7.93×10^{-5}	214	3.67×10^{-7}
	Custom 450	25	−285	315	3.02×10^{-4}	5.82×10^{-4}	485	3.70×10^{-4}
		49	−223	536	1.86×10^{-4}	3.46×10^{-4} *	673 *	2.58×10^{-4}
	AM350	25	−258	906	3.13×10^{-4}	5.41×10^{-4} *	1049 *	3.09×10^{-4}
		49	−231	921	2.61×10^{-4}	5.52×10^{-4} *	1038 *	3.71×10^{-4}

* pseudo-passivation.

Table 5. Electrochemical parameters obtained from PPC by PHSS passivated in citric acid at 90 min exposure to H_2SO_4 and NaCl solutions.

Solution	PHSS	Temp. (°C)	E_{corr} (mV)	E_{pit} (mV)	i_{corr} (mA/cm^2)	i_{pass} (mA/cm^2)	Range Passive (mV)	Corrosion Rate (mm/y)
H_2SO_4	15-5PH	25	−329	831	1.30×10^{-3}	6.43×10^{-3}	621	6.41×10^{-5}
		49	46	601	3.87×10^{-5}	1.87×10^{-3}	718	6.91×10^{-6}
	17-4PH	25	−296	815	1.39×10^{-2}	7.27×10^{-3}	761	1.12×10^{-4}
		49	−352	819	2.85×10^{-3}	6.24×10^{-3}	692	9.00×10^{-5}
	Custom 450	25	−279	936	2.97×10^{-3}	7.42×10^{-3}	722	1.31×10^{-2}
		49	−241	937	5.36×10^{-3}	5.14×10^{-3}	758	2.58×10^{-2}
	AM350	25	−288	874	1.22×10^{-3}	7.34×10^{-3}	698	2.46×10^{-2}
		49	−360	882	4.78×10^{-3}	5.41×10^{-3}	596	2.11×10^{-3}
NaCl	15-5PH	25	−291	116	4.53×10^{-5}	1.04×10^{-4}	319	4.46×10^{-7}
		49	−239	425	4.34×10^{-5}	1.23×10^{-4}	312	4.75×10^{-7}
	17-4PH	25	−200	275	8.75×10^{-5}	2.52×10^{-4} *	433 *	9.12×10^{-7}
		49	−275	400	6.43×10^{-5}	2.01×10^{-4} *	355 *	5.63×10^{-7}
	Custom 450	25	−285	315	3.02×10^{-4}	9.81×10^{-4} *	422 *	6.26×10^{-4}
		49	−223	536	1.86×10^{-4}	1.08×10^{-3}	445	5.74×10^{-4}
	AM350	25	−258	906	3.13×10^{-4}	8.09×10^{-4} *	351 *	6.95×10^{-4}
		49	−231	921	2.61×10^{-4}	8.78×10^{-4} *	1048 *	8.95×10^{-4}

* pseudo-passivation.

Figure 5a–d shows the PPC for passivated PHSS samples in citric acid at 25 and 49 °C for 60 min and exposure to sulfuric acid and sodium chloride solutions. The anodic and cathodic branches presented activation in a range of 500 mV. The corrosion potential (E_{corr}) in most cases was around −400 mV. However, the corrosion potential in sodium chloride at 25 °C is −600 mV. All the passivated samples resulted in a stable passivation range in both solutions, being larger for the samples exposed to the sulfuric acid solution at 25 and 49 °C. Under these conditions, the samples continued with the second passivation. AM 350 steel presented a pseudo-passivation followed by transpassivation in the sodium chloride solution. The corrosion current densities (i_{corr}) for the PHSS samples in the sulfuric acid solution were found at 10^{-3} mA/cm^2, and for the sodium chloride solution at 10^{-4} mA/cm^2, respectively. Such behaviors occurred in PHSS passivated with citric acid, i.e., a strong acid obtained from citrus fruits, in order to have an "eco-friendly" passivation treatment [28,50].

Figure 6a–d shows the CPPs obtained for PHSS from bath nitric acid at 25 and 49 °C for 60 min, exposing the passivated PHSS to sulfuric acid or sodium chloride solutions. Nitric is a strong acid that, with an increasing temperature of around 83 °C, can generate toxic nitrate vapors harmful to health. The anodic and cathodic branches present activation in a range of 500 mV. However, the cathode branches of the PHSS samples exposed to a sodium chloride solution present a concentration polarization effect. The E_{corr} of the anodic branch varies from 300 to 200 mV, with 15-5PH being at nobler potentials, also at a temperature of 49 °C either in sulfuric acid or sodium chloride solutions. The formation of the passive layer is variable. In sulfuric acid, there is even secondary passivation. In contrast, in a sodium chloride solution, there is the activation of the system followed by a small passive layer of 200 mV. The i_{corr} for the PHSS samples in sulfuric acid solution was found at 10^{-3} mA/cm^2 and for the sodium chloride solution at 10^{-4} and 10^{-5} mA/cm^2, respectively.

Table 6. Electrochemical parameters obtained by PPC for PHSS passivated in nitric acid at 90 min exposure to H_2SO_4 and NaCl solutions.

Solution	PHSS	Temp. (°C)	E_{corr} (mV)	E_{pit} (mV)	i_{corr} (mA/cm^2)	i_{pass} (mA/cm^2)	Range Passive (mV)	Corrosion Rate (mm/y)
H_2SO_4	15-5PH	25	−320	844	1.66×10^{-3}	7.37×10^{-3}	813	1.65×10^{-4}
		49	72	901	5.64×10^{-5}	4.65×10^{-3} *	752 *	7.07×10^{-7}
	17-4PH	25	−418	860	2.11×10^{-2}	1.92×10^{-3}	715	5.19×10^{-6}
		49	−377	800	1.54×10^{-3}	3.13×10^{-4}	562	5.31×10^{-7}
	Custom 450	25	−305	934	3.91×10^{-3}	5.48×10^{-3}	883	1.65×10^{-2}
		49	−314	899	1.86×10^{-3}	6.38×10^{-3}	911	1.23×10^{-2}
	AM350	25	−307	895	1.29×10^{-3}	4.93×10^{-3}	735	1.24×10^{2}
		49	−327	737	1.33×10^{-3}	7.88×10^{-3}	847	1.22×10^{-2}
NaCl	15-5PH	25	−238	426	4.14×10^{-5}	6.48×10^{-5}	288	2.60×10^{-7}
		49	−227	739	3.47×10^{-5}	5.53×10^{-5}	217	2.39×10^{-7}
	17-4PH	25	−206	285	8.33×10^{-5}	1.14×10^{-4}	259	5.10×10^{-7}
		49	−282	269	6.23×10^{-5}	1.17×10^{-4} *	452 *	4.61×10^{-7}
	Custom 450	25	−247	260	2.27×10^{-4}	4.43×10^{-4} *	405 *	4.01×10^{-4}
		49	−248	777	1.95×10^{-4}	3.31×10^{-4}	212	4.45×10^{-4}
	AM350	25	−257	417	3.38×10^{-4}	7.22×10^{-4} *	558 *	3.89×10^{-4}
		49	−250	522	2.56×10^{-4}	5.39×10^{-4} *	671 *	5.62×10^{-4}

* pseudo-passivation.

The electrochemical parameters obtained from the potentiodynamic polarization of the materials passivated in citric acid can be seen in Tables 3 and 4, where the steel is exposed to a sulfuric acid solution forming more stable layers followed by transpassivation and secondary passivation. The values of the passivation range showed only a tendency in the PHSS steels (marked with the symbol *) since it was not completely defined.

Pitting potential (E_{pit}) is the potential value at which the current increases and the pitting attack occurs. The passivated PHSS in citric and nitric acid at 60 min had pitting potential values from 45 mV (15-5 PH) to 921 mV (AM350) in NaCl solution and values from 586 mV (AM350) to 937 mV (Custom 450) in H_2SO_4 solution, respectively.

Figure 7a–d shows the potentiodynamic polarization curves of the passivated PHSS in a nitric acid bath at 25 and 49 °C for 90 min and exposing the passivated PHSS to a sulfuric acid or sodium chloride solution. The anodic and cathodic branches presented activation in a range of 600 mV. The corrosion potential of these steels is around −300 mV. 15-5 PH steel has a corrosion potential (E_{corr}) value of −20 mV in sulfuric acid solution at 49 °C. The PHSS samples exposed to sulfuric acid solution have a stable passivation range that goes from −200 to 800 mV, followed by a transpassivation, and the samples in sodium chloride solution have an unstable passivation range because they present a pseudo-passivation at both temperatures. The passivated PHSS have current densities (i_{corr}) of 10^{-3} mA/cm^2 in sulfuric acid solution and 10^{-4} and 10^{-5} mA/cm^2 in sodium chloride solution.

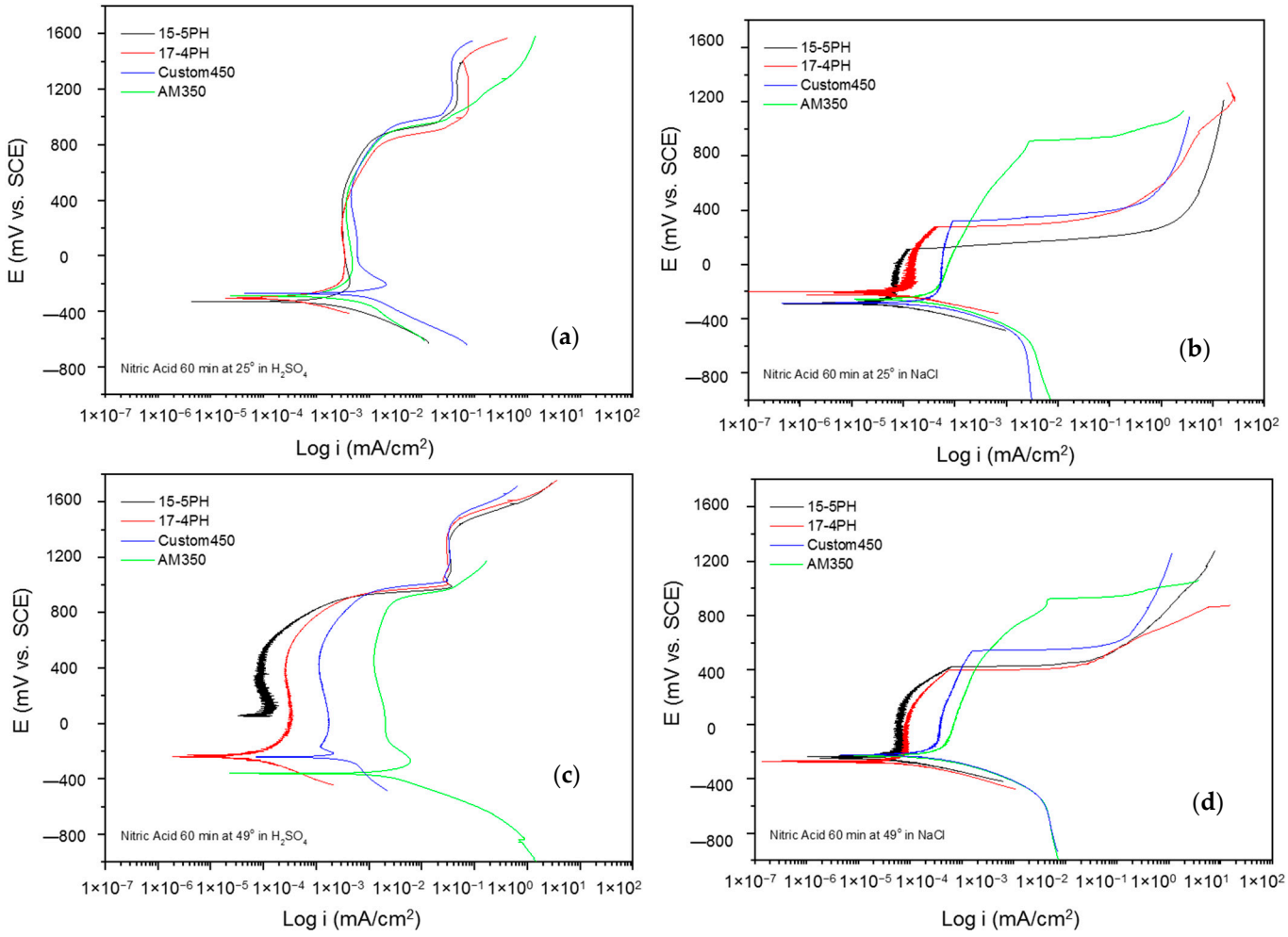

Figure 7. Potentiodynamic polarization curves for passivated PHSS in nitric acid, at 25 and 49 °C for 60 min: (**a**,**c**) H_2SO_4 and (**b**,**d**) NaCl solutions.

Figure 8a–d shows the potentiodynamic polarization curves of the passivated PHSS in a bath of nitric acid at 25 and 49 °C for 90 min and exposing the passivated PHSS to sulfuric acid or sodium chloride solutions. The anodic and cathodic branches present activation in a range of 500 mV. A concentration polarization effect is observed in the cathode branches of the samples exposed to sodium chloride solution. The E_{corr} range of −200 to −400 mV for all samples. The PHSS samples passivated in citric and nitric acid present the same behavior when exposed to sulfuric acid and sodium chloride solutions. Passivation ranges are stable, followed by transpassivation and secondary passivation when samples are in sulfuric acid. They have an unstable passivation range when exposed to sodium chloride because they present a pseudo-passivation at both temperatures. The i_{corr} for the PHSS samples in sulfuric acid solution was found at 10^{-3} mA/cm^2, and for the sodium chloride solution at 10^{-4} and 10^{-5} mA/cm^2, respectively.

The electrochemical parameters obtained from the potentiodynamic polarization of PHSS passivated in nitric acid are presented in Tables 5 and 6. The values of the passivation range showed only a tendency in the PHSS steels (marked with the symbol *) since it was not completely defined. The corrosion potential ranges from −400 to 70 mV, where the noblest values occur at higher passivation temperatures and in sulfuric acid. The pitting potential was above 700 mV in the sulfuric acid solution, while sodium chloride was above 300 mV. Current densities (i_{corr}) are of the order of 10^{-3} mA/cm^2 in sulfuric acid medium and 10^{-3} mA/cm^2 in sodium chloride.

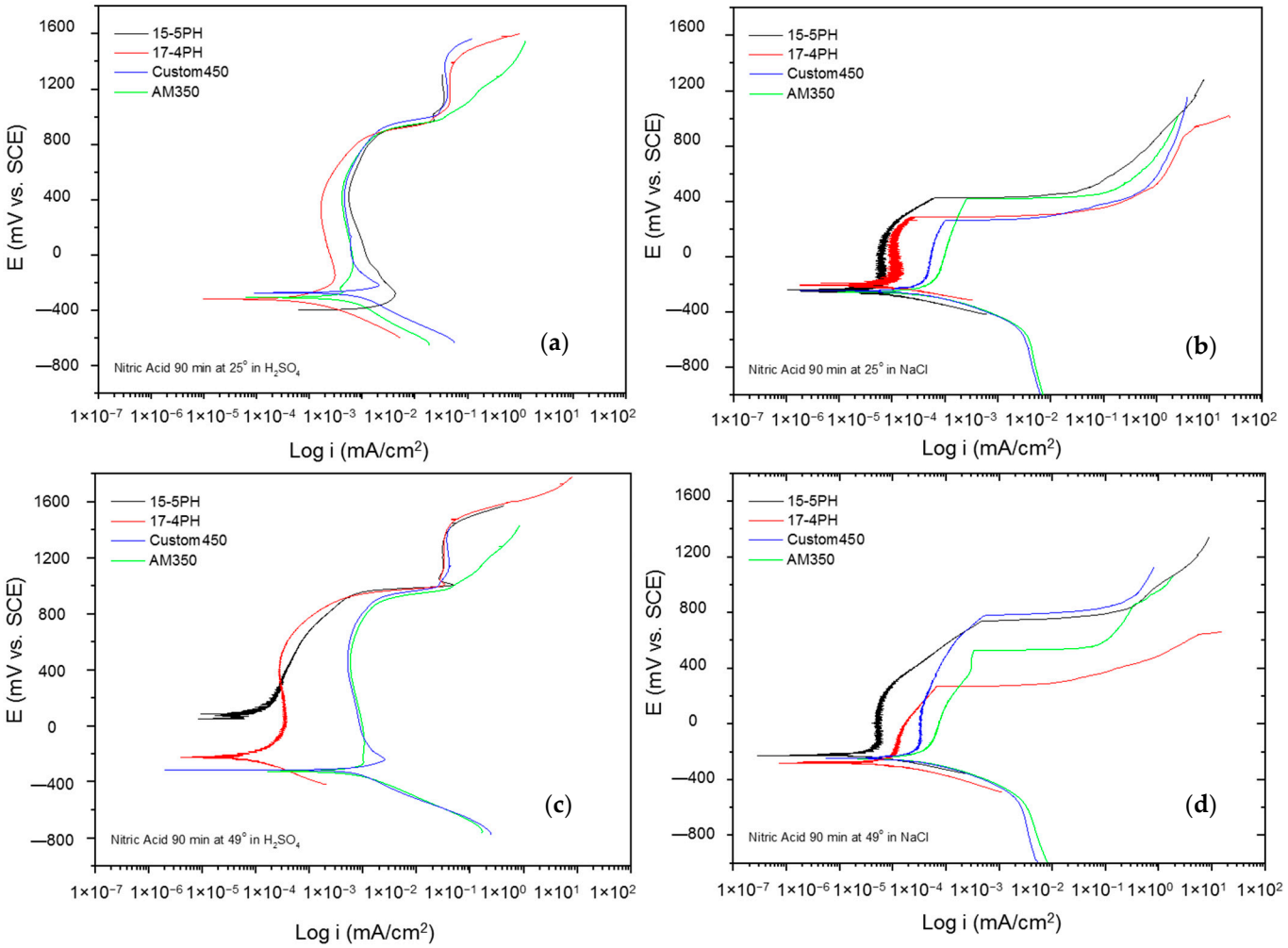

Figure 8. Potentiodynamic polarization curves for passivated PHSS in nitric acid, at 25 and 49 °C for 90 min: (**a**,**c**) H_2SO_4 and (**b**,**d**) NaCl solutions.

The current results of the potentiodynamic polarization curves of the passivated PHSS in nitric acid bath acid at 25 and 49 °C for 60 and 90 min and exposure to solutions of sulfuric acid and sodium chloride allowed us to find out the behavior of the corrosion kinetics of precipitation hardening stainless steels. Hence, mixed activation and passivation (formation of a passive film) was shown, followed by a transpassivation or secondary passivation trend. In the PPC, more stable passivation was observed in sulfuric acid solution, and pseudo-passivation when the steels were exposed to sodium chloride solution.

The shapes of the potentiodynamic polarization curves (Figures 5–8) of the PHSS steels are different, which indicates since the electrochemical processes were not similar in NaCl and H_2SO_4 test solutions, there is passivation in the anodic reaction, but their pitting potential is different. However, two characteristic mechanisms are present in the potentiodynamic polarization curves when the PHSS is immersed in the H_2SO_4 solution. This passivation protection mechanism occurs when the passivation film formed on the surface of the Cr-Fe alloy determines its corrosion resistance. Chromium oxides play an important role in passive films, and the behavior is attributed to the anodic reactions of the OH^-. The increase in the current density in the PHSS samples gives rise to the transpassivation and formation of secondary passivation. In the case of samples immersed in NaCl solution, there is a pseudo-passivation not representing stable passivation film. This protection mechanism occurs due to the formation of a passive layer formed by oxides and oxy/hydroxides rich in Cr that prevents the propagation of oxygen to the internal

layer and protects the base material from the penetration of corrosive ions such as the Cl- to which the samples were exposed [50–54].

Gaona et al. [29] indicate that the corrosion kinetics of stainless steels are associated with an increase in current density as a result of an unstable passivation film when the samples are immersed in NaCl solution. However, austenitic stainless steels immersed in H_2SO_4 solution showed transients associated with rupture of the passivation film (transpassivation) and regeneration of the passive layer (secondary passivation).

Research by Lara et al., Samaniego et al., Noh et al., and Gaydos et al. [13,16,23,55,56] have indicated that stainless steels passivated in nitric acid showed a higher trend of pitting corrosion, concluding that nitric acid increases the chromium presence of the passive layer, removing MnS inclusions from the surface. The probability of individual pitting also increases. In this research, the samples passivated in nitric acid presented more corrosion than those passivated within citric acid due to the presence of MnS. To reduce the presence of MnS, changes in the acid concentration or the use of other solutions similar to citric acid, where the pitting process was more controlled, should be used. See Equations (2) and (3). From the above reactions, MnS can be removed, and the passivation stability could be related to the acid concentration.

$$MnS + 2H^+ \rightarrow Mn^{2+} + H_2S \quad (2)$$

$$2MnS + 3H_2O \rightarrow 2Mn^{2+} + S_2O_3^{2-} + 6H^+ + 8e^- \quad (3)$$

According to some authors [57–59], the results indicated that during passivation in the PHSS, there is a relatively stable range of passive potential. The passive current density is the same, which indicates that it forms a relatively stable passive film. However, if the electrochemical process is still active in the anodic reaction, the passive current density is not the same, and the passive film is unstable.

Some authors say stainless steels present passive films before and after transpassivation [60,61]. Transpassivation is a dissolution mechanism where the steel is activated and begins to dissolve, having noble electrode potentials [62,63]. A characteristic of passivated stainless steel is that passivation occurs in the anodic branch. This is where most of the studies have been focused on, forgetting that some acid solutions can cause a second film for passivation, as observed in this study.

The passive zone involves the formation of chromium and iron oxide films that is commonly present in PHSS [28,64–66]. Hence, selective dissolution on the surface of stainless steels generates the presence of Cr^{3+}, leading to the formation of the chromium trihydroxide compound $Cr(OH)_3$ (see Equation (4)). When $Cr(OH)_3$ is on the surface, and the hydroxides continue to react, the dissolution leads to the formation of a continuous passive film of chromium oxide Cr_2O_3 (see Equation (5)) [28,67,68].

$$Cr^{3+} + 3OH^- \rightarrow Cr(OH)_3 + 3e^- \quad (4)$$

$$Cr(OH)_3 + Cr + 3OH^- \rightarrow Cr_2O_3 + 3H_2O + 3e^- \quad (5)$$

As mentioned before, the anodic reactions during the passivation film growth period come mainly from the oxidation of iron and chromium. The oxidation reactions of iron can be seen in Equations (6)–(8) [69–72]:

$$3Fe + 8OH^- \rightarrow Fe_3O_4 + 4H_2O + 8e^- \quad (6)$$

$$2Fe_3O_4 + 2OH^- + 2H_2O \rightarrow 6FeOOH + 2e^- \quad (7)$$

$$2Fe_3O_4 + 2OH^- \rightarrow 3Fe_2O_3 + H_2O + 2e^- \quad (8)$$

Pseudo-passivation occurred in the passivated samples of PHSS immersed in 3.5 wt.% NaCl. The current density continues to increase with increases in the anodic potential instead of reaching the stable state within the passive region, thus suggesting that the

passive films formed on the PHSS are in an incomplete steady state. Chloride ions (Cl^-) cause this instability since they have a great ability to adhere to the steel surface and then diffuse into the steel through defects in the passive surface film, thus impairing the effectiveness of the passive film of the PHSS [23,28,73,74]. The pseudo-passivation phenomenon observed in the different passivated samples in the polarization curve may be associated with the formation of the $Cr(OH)_3$ film, and the rupture of the pseudo-passivation is accompanied by the detachment of the $Cr(OH)_3$ film. Therefore, the $Cr(OH)_3$ film functions as a pseudo-passive film [75,76]. As some papers have reported, $Cr(OH)_3$ could block the path of the dissolution of the iron, isolate the corrosion media and reduce the number of active sites of the iron dissolution [77,78].

The schematic diagram shows the corrosion mechanism for 15-5PH, 17-4PH, CUSTOM 450, and AM 350 stainless steels after the passivation process in $C_6H_8O_7$ and HNO_3 baths (see Figure 9). The passive protective film formed on stainless steel surfaces is highly attributed to the corrosion resistance in these steels. The double-layer structure of SS passive film has a double-layer structure that is rich in Fe and Cr, respectively. Chromium oxides play a significant role in the corrosion resistance of PHSS. Cr^{3+} has higher anticorrosion stability compared to FeO and Fe_2O_3 oxides. Therefore, the Cr_2O_3 content in the stainless steel passive film is a primary factor for the stability and anticorrosive property of the steel. Defects will form in the passive film, leading to the nucleation of localized corrosion (generating pitting). On the other hand, the defect density of the iron-rich outer layer is higher than that of the chromium-rich inner layer, which could lead to the absorption of a large amount of Cl^- in the passive film in PHSS [13,29,79,80]. In Figure 9a, the protection mechanism occurs due to the formation of a passive layer formed by oxides and oxy/hydroxides rich in Cr that prevents the propagation of oxygen to the internal layer and protects the base material from the penetration of corrosive ions such as the Cl^- to which the samples were exposed. In the case of Figure 9b, the protection mechanism is different since passivation occurs. The passivation film formed on the surface of the Cr–Fe alloy determined its corrosion resistance. Chromium oxides play an important role in passive films [81].

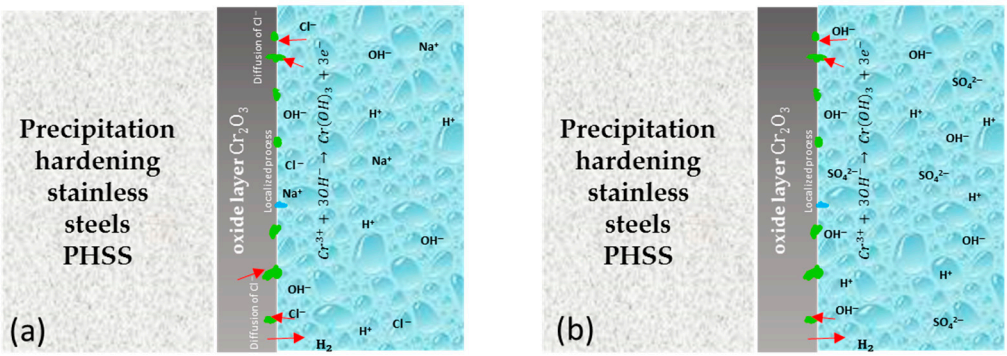

Figure 9. Schematic diagram of passivation treatment in citric and nitric acid baths for 15-5PH, 17-4PH, CUSTOM 450, and AM 350 stainless steels exposed to (**a**) 5 wt.% NaCl solution; (**b**) 1 wt.% H_2SO_4 solution.

According to the literature [16,28,29,82–87], citric acid can be an alternative to nitric acid since citric acid passivation indicates better results than the nitric acid solution. Furthermore, samples passivated within citric acid presented a lower trend to localized corrosion.

4. Conclusions

This research shows the passive state of PHSS passivated in acid baths at 25 and 49 °C for 60 and 90 min and immersed in NaCl and H_2SO_4 solutions. From these results, the following can be concluded:

- OM characterization indicated that the martensitic PHSS presented a microstructure with a martensitic (α') phase and a semi-austenitic PHSS containing a microstructure

of austenite (γ) and delta (δ) ferrite phases, respectively. Based on the values obtained from PREN, the AM 350 (semi-austenitic) (29.80) presented a higher corrosion resistance than the martensitic 15-5 PH (23.5), 17-4 PH (17.5), and CUSTOM 450 (20.9).

- Potentiodynamic polarization results allowed us to determine the corrosion kinetic behavior of PHSS passivated samples immersed in H_2SO_4 and NaCl solutions and passivity in the anodic branch.
- The current density levels in NaCl solution were between 10^{-4} and 10^{-5} mA/cm^2, while those of H_2SO_4 were recorded around 10^{-2} and 10^{-3} mA/cm^2.
- Using the citric acid bath as a substitute for nitric acid in the passivation process generates a system in which the electrochemical behavior is similar, mixed by activation, where the anodic branch presents a series of events such as pseudo-passivation and/or passivation–transpassivation–secondary passivation.
- PHSS passivated in nitric acid and immersed in sodium chloride have higher pitting potentials than samples passivated in citric acid.
- The citric acid passivation treatment on PHSS could be a green alternative to the currently employed nitric acid passivation treatment because it is not toxic and is friendly to the environment.
- Based on the results obtained from the corrosion behavior of passivated PHSS, it is considered that future work may use electrochemical impedance spectroscopy to analyze and complement the corrosion mechanism and characterize the oxides through the XPS technique.

Author Contributions: Conceptualization, J.V.-T., C.G.-T. and F.A.-C. methodology, J.V.-T., E.M.-B., M.L.-B., F.E.-L. and C.G.-T.; data curation, F.A.-C., J.C.-M., D.N.-M., F.A.-C., J.O.-C. and F.E.-L.; formal analysis, F.A.-C., M.A.B.-Z. and C.G.-T.; writing—review and editing, F.A.-C., E.M.-B. and C.G.-T. All authors have read and agreed to the published version of the manuscript.

Funding: This research received no external funding.

Acknowledgments: The authors would like to thank the UANL-CA-316 working group and Universidad Autónoma de Nuevo León (UANL) for the facilities given to developing this investigation.

Conflicts of Interest: The authors declare no conflict of interest.

References

1. Mouritz, P.A. *Introduction to Aerospace Materials*; Woodhead Publishing: Cambridge, UK, 2012.
2. Gloria, A.; Montanari, R.; Richetta, M.; Varone, A. Alloys for aeronautic applications: State of the art and perspectives. *Metals* **2019**, *9*, 662. [CrossRef]
3. Martinez, B.; Tiburcio, C.G.; Bastidas, D.; Lara-Banda, M.; Samaniego, O.; Calderon, F.A. Electrochemical Evaluation of 15-5PH Stainless Steel Passivated in Citric Acid. *ECS Trans.* **2022**, *106*, 223. [CrossRef]
4. Lopes, J.C. Material selection for aeronautical structural application. *Sci. Technol. Adv. Mater.* **2008**, *20*, 78–82.
5. Lo, K.H.; Shek, C.H.; Lai, J.K.L. Recent developments in stainless steels. *Mater. Sci. Eng. R.* **2009**, *65*, 39–104. [CrossRef]
6. Lara Banda, M.; Gaona-Tiburcio, C.; Zambrano-Robledo, P.; Cabral, M.J.A.; Estupinan, F.; Baltazar-Zamora, M.A.; Almeraya-Calderon, F. Corrosion Behaviour of 304 Austenitic, 15-5PH and 17-4PH Passive Stainless Steels in acid solutions. *Int. J. Electrochem. Sci.* **2018**, *13*, 10314–10324. [CrossRef]
7. Gialanella, S.; Malandruccolo, A. *Aerospace Alloys*; Topics in Mining, Metallurgy and Materials Engineering; Bergmann, C.P., Ed.; Springer: Cham, Switzerland, 2020; ISSN 2364-3307. [CrossRef]
8. Cobb, H.M. *The History of Stainless Steel*; ASM International: Cleveland, OH, USA, 2010; pp. 189–192.
9. Ha, H.Y.; Jang, J.H.; Lee, T.H.; Won, C.; Lee, C.H.; Moon, J.; Lee, C.G. Investigation of the localized corrosion and passive behavior of type 304 stainless steels with 0.2–1.8 wt% B. *Materials* **2018**, *11*, 2097. [CrossRef]
10. Schmuki, P. From bacon to barriers: A review on the passivity of metal and alloys. *J. Solid State Electr.* **2002**, *6*, 145–164. [CrossRef]
11. Dong, H.; Esfandiari, M.; Li, X.Y. On the microstructure and phase identification of plasma nitrided 17-4PH precipitation hardening stainless steel. *Surf. Coat. Technol.* **2008**, *202*, 2969–2975. [CrossRef]
12. Hsiao, C.N.; Chiou, C.S.; Yang, J.R. Aging reactions in a 17-4 PH stainless steel. *Mater. Chem. Phys.* **2002**, *74*, 134–142. [CrossRef]
13. Samaniego-Gámez, O.; Almeraya-Calderón, F.; Chacón-Nava, J.; Maldonado-Bandala, E.; Nieves-Mendoza, D.; Flores-De los Rios, J.P.; Gaona-Tiburcio, C. Corrosion Behavior of Passivated CUSTOM450 and AM350 Stainless Steels for Aeronautical Applications. *Metals* **2022**, *12*, 666. [CrossRef]
14. Gladman, T. Precipitation hardening in metals. *Mater. Sci. Technol.* **1999**, *15*, 30–36. [CrossRef]

15. Farrar, J. *The Alloy Tree—A Guide to Low-Alloy Steels, Stainless Steels and Nickel-base Alloys*; Woodhead Publishing Limited and CRC Press: Sawston, UK, 2004.
16. Gaydos, S.P. Passivation of aerospace stainless parts with citric acid solutions. *Plat. Surf. Finish.* **2003**, *90*, 20–25.
17. *ASTM A967-17*; Standard Specification for Chemical Passivation Treatments for Stainless Steel Parts. ASTM International: West Conshohocken, PA, USA, 1999.
18. Shibata, T. Stochastic studies of passivity breakdown. *Corros. Sci.* **1990**, *31*, 413–423. [CrossRef]
19. Ashassi-Sorkhabi, H.; Seifzadeh, D.; Raghibi-Boroujeni, M. Analysis of electrochemical noise data in both time and frequency domains to evaluate the effect of ZnO nanopowder addition on the corrosion protection performance of epoxy coatings. *Arab. J. Chem.* **2016**, *9*, S1320–S1327. [CrossRef]
20. El-Taib Heakal, F.; Ameer, M.A.; El-Aziz, A.M.; Fekry, A.M. Electrochemical behavior of Mo-containing austenitic stainless steel in buffer solutions. *Mater. Werkstofftech.* **2004**, *35*, 407–413. [CrossRef]
21. El-Taib Heakal, F.; Ghoneim, A.; Fekry, A. Stability of spontaneous passive films on high strength Mo-containing stainless steels in aqueous solutions. *J. Appl. Electrochem.* **2007**, *37*, 405–413. [CrossRef]
22. Ameer, M.A.; Fekry, A.M.; El-TaibHeakal, F. Electrochemical behaviour of passive films on molybdenum-containing austenitic stainless steels in aqueous solutions. *Electrochim. Acta* **2004**, *50*, 43–49. [CrossRef]
23. Lara-Banda, M.; Gaona-Tiburcio, C.; Zambrano-Robledo, P.; Delgado-E, M.; Cabral-Miramontes, J.A.; Nieves-Mendoza, D.; Maldonado-Bandala, E.; Estupiñan-López, F.; Chacón-Nava, J.G.; Almeraya-Calderón, F. Alternative to nitric acid passivation of 15-5 and 17-4PH stainless steel using electrochemical techniques. *Materials* **2020**, *13*, 2836. [CrossRef]
24. Bragaglia, M.; Cherubini, V.; Cacciotti, I.; Rinaldi, M.; Mori, S.; Soltani, P.; Nanni, F.; Kaciulis, S.; Montesperelli, G. Citric Acid Aerospace Stainless Steel Passivation: A Green Approach. In Proceedings of the CEAS Aerospace Europe Conference 2015, Delft, The Netherlands, 7–11 September 2015.
25. Marcelin, S.; Pébèrea, N.; Régnierb, S. Electrochemical characterisation of a martensitic stainless steel in a neutral chloride solution. *Electrochim. Acta* **2013**, *87*, 32–40. [CrossRef]
26. Mollapour, Y.; Poursaeidi, E. Experimental and numerical analysis of Pitting Corrosion in CUSTOM 450 Stainless Steel. *Eng. Fail. Anal.* **2021**, *128*, 105589. [CrossRef]
27. Lin, C.K.; Chu, C.C. Mean stress effects on low-cycle fatigue for a precipitation-hardening martensitic stainless steel in different tempers. *Fatigue Fract. Eng. Mater. Struct.* **2000**, *23*, 545–553. [CrossRef]
28. Almeraya-Calderón, F.; Samaniego-Gámez, O.; Maldonado-Bandala, E.; Nieves-Mendoza, D.; Olguín-Coca, J.; Jáquez-Muñoz, J.M.; Cabral-Miramontes, J.; Flores-De los Rios, J.P.; Bautista-Margulis, R.G.; Gaona-Tiburcio, C. Corrosion Behavior of Passivated Martensitic and Semi-Austenitic Precipitation Hardening Stainless Steel. *Metals* **2022**, *12*, 1033. [CrossRef]
29. Gaona Tiburcio, C.; Samaniego-Gámez, O.; Jáquez-Muñoz, J.; Baltazar-Zamora, M.A.; Landa-Ruiz, L.; Lira-Martínez, A.; Flores-De los Rios, J.P.; Cabral-Miramontes, J.; Estupinán-López, F.; Almeraya-Calderon, F. Frequency-Time Domain Analysis of Electrochemical Noise of Passivated AM350 Stainless Steel for Aeronautical Applications. *Int. J. Electrochem. Sci.* **2022**, *17*, 220950. [CrossRef]
30. Custom 450® Stainless Steel. Available online: https://www.ulbrich.com/uploads/data-sheets/Custom-450-Stainless-Steel-Wire-UNS-S45000.pdf (accessed on 30 April 2022).
31. 15-5PH Stainless | AMS5659. (s. f.). Available online: https://www.smithsadvanced.com/15-5ph-stainless (accessed on 7 November 2022).
32. CIVMATS CO., Ltd. 17-4PH Stainless Steel-Introduction, Applications, Data Sheet. civmats.com. Available online: https://www.civmats.com/grades/GRADES-17-4PH.HTML (accessed on 7 November 2022).
33. AM 350 Technical Data. Available online: https://www.hightempmetals.com/techdata/hitempAM350data.php (accessed on 29 September 2022).
34. *ASTM A380-17*; Standard Practice for Cleaning, Descaling and Passivation of Stainless-Steel Parts, Equipment, and Systems. ASTM International: West Conshohocken, PA, USA, 1999.
35. *ASTM E3-95*; Standard Practice for Preparation of Metallographic Specimens. ASTM International: West Conshohocken, PA, USA, 1995.
36. *SAE AMS 2700F*; Passivation of Corrosion Resistant Steels. Aerospace Material Specification. SAE International: Warrendale, PA, USA, 2018.
37. *ASTM G5-11*; Standard Reference Test Method for Making Potentiostatic and Potentiodynamic Anodic Polarization Measurements. ASTM International: West Conshohocken, PA, USA, 2011.
38. Jaquez-Muñoz, J.; Gaona-Tiburcio, C.; Lira-Martinez, A.; Zambrano-Robledo, P.; Maldonado-Bandala, E.; Samaniego-Gamez, O.; Nieves-Mendoza, D.; Olguin-Coca, J.; Estupiñan-Lopez, F.; Almeraya-Calderon, F. Susceptibility to pitting corrosion of Ti-CP2, Ti-6Al-2Sn-4Zr-2Mo, and Ti-6Al-4V alloys for aeronautical applications. *Metals* **2021**, *11*, 1002. [CrossRef]
39. Montoya-Rangel, M.; de Garza-Montes, O.N.; Gaona-Tiburcio, C.; Colás, R.; Cabral-Miramontes, J.; Nieves-Mendoza, D.; Maldonado-Bandala, E.; Chacón-Nava, J.; Almeraya-Calderón, F. Electrochemical Noise Measurements of Advanced High-Strength Steels in Different Solutions. *Metals* **2020**, *10*, 1232. [CrossRef]
40. Cabral-Miramontes, J.A.; Bastidas, M.D.; Baltazar, M.A.; Zambrano-Robledo, P.; Bastidas, J.M.; Almeraya-Calderón, F.; Gaona-Tiburcio, C. Corrosion behavior of Zn-TiO_2 and Zn-ZnO Electrodeposited Coatings in 3.5% NaCl solution. *Int. J. Electrochem. Sci.* **2019**, *14*, 4226–4239. [CrossRef]

41. Abedi, H.R.; Hanzaki, A.Z.; Haghdadi, N.; Hodgson, P.D. Substructure induced twinning in low density steel. *Scr. Mater.* **2017**, *128*, 69–73. [CrossRef]
42. Gupta, A.; Bhargava, A.K.; Tewari, R.; Tiwari, A.N. TEM studies of boron-modified 17Cr-7Ni precipitation-hardenable stainless steel via rapid solidification route. *Metal. Mater. Trans. A* **2013**, *44*, 4248–4256. [CrossRef]
43. Xu, X.L.; Yu, Z.W. Metallurgical analysis on a bending failed pump-shaft made of 17-7PH precipitation-hardening stainless steel. *J. Mater. Process. Technol.* **2008**, *198*, 254–259. [CrossRef]
44. Ramirez-Arteaga, A.M.; Gonzalez-Rodriguez, J.G.; Campillo, B.; Gaona-Tiburcio, C.; Dominguez-Patiño, G.; Leduc Lezama, L.; Chacon-Nava, J.G.; Neri-Flores, M.A.; Martinez-Villafañe, A. An electrochemical study of the corrosion behavior of a dual phase steel in 0.5 m H_2SO_4. *Int. J. Electrochem. Sci.* **2010**, *5*, 1786–1798.
45. The British Stainless Steel Association 2022. Available online: https://bssa.org.uk/bssa_articles/calculation-of-pren/ (accessed on 2 June 2022).
46. Schweitzer, P. *Fundamentals of Metallic Corrosion: Atmospheric and Media Corrosion of Metals*; CRC Press Taylor & Francis Group: Boca Raton, FL, USA, 2007; ISBN 10:0-8493-8243-2.
47. Olsson, C.-O.A. Wet Corrosion of Stainless Steels and Other Chromium-Bearing Alloys. In *Encyclopedia of Interfacial Chemistry*; Surface Science and Electrochemistry; Elsevier: Bonn, Germany, 2018; pp. 535–542. [CrossRef]
48. Tafel, J. Über die Polarisation bei kathodischer Wasserstoffentwicklung. *Z. Für Phys. Chem.* **1905**, *50*, 641–712. [CrossRef]
49. Butler, J.A.V. Studies in heterogeneous equilibria. Part II.—The kinetic interpretation on the Nernst theory of electromotive force. *Trans. Faraday Soc.* **1924**, *19*, 729–733. [CrossRef]
50. Bojinov, M.; Fabricius, G.; Laitinen, T.; Saario, T. The mechanism of the transpassive dissolution of chromium in acidic sulfate solutions. *J. Electrochem. Soc.* **1998**, *145*, 2043–2050. [CrossRef]
51. Tian, H.; Sun, F.; Chu, F.; Wang, L.; Wang, X.; Cui, Z. Passivation behavior and surface chemistry of 316 SS in the environment containing Cl^- and NH_4^+. *J. Electroanal. Chem.* **2021**, *886*, 115138. [CrossRef]
52. Zhu, Z.; Zhang, Q.; Liu, P.; Zhang, J.; Cao, F. Quasi-simultaneous electrochemical/chemical imaging of local Fe^{2+} and pH distributions on 316 L stainless steel surface. *J. Electroanal. Chem.* **2020**, *871*, 114107. [CrossRef]
53. Duan, Z.; Man, C.; Dong, C.; Cui, Z.; Kong, D.; Wang, L.; Wang, X. Pitting behavior of SLM 316L stainless steel exposed to chloride environments with different aggressiveness: Pitting mechanism induced by gas pores. *Corros. Sci.* **2020**, *167*, 108520. [CrossRef]
54. Noh, L.S.; Laycock, N.J.; Gao, W.; Wells, D.B. Effects of nitric acid passivation on the pitting resistance of 316 stainless steel. *Corros. Sci.* **2000**, *42*, 2069–2084. [CrossRef]
55. Brossia, C.S.; Kelly, R.G. On the role of alloy sulfur in the initiation of crevice corrosion in stainless steel. In *Critical Factors in Localized II*; Natishan, P.M., Kelly, R.G., Frankel, G.S., Newman, R.C., Eds.; The Electrochemical Society: Pennington, NJ, USA, 1996; Volumes 95–115, pp. 201–217.
56. Doh, S.J.; Je, J.H.; Kim, J.S.; Kim, K.Y.; Kim, H.S.; Lee, Y.D.; Lee, J.M.; Hwu, Y. Influence of Cr and Mo on the passivation of stainless steel430 (18Cr) and 444 (18Cr–2Mo): In situ XANES study. *Nucl. Instrum. Methods B* **2003**, *199*, 211–215. [CrossRef]
57. Choudhary, S.; Qiu, Y.; Thomas, S.; Birbilis, N. Element-resolved electrochemical analysis of transpassive dissolution and repassivation behavior of the multi-principal element alloy AlTiVCr. *Electrochim. Acta* **2020**, *362*, 137104. [CrossRef]
58. Li, Z.X.; Zhang, L.M.; Udoh, I.I.; Ma, A.L.; Zheng, Y.G. Deformation-induced martensite in 304 stainless steel during cavitation erosion: Effect on passive film stability and the interaction between cavitation erosion and corrosion. *Tribol. Int.* **2022**, *167*, 107422. [CrossRef]
59. Zhang, L.; Qi, L.; Deng, S.; Oguntuase, O.; Deng, T.; Wang, H.; Ojo, A. Analyses of Anodically Formed Passive Film and Corrosion Behavior of Wire-arc Additive Manufactured ATI 718Plus® Superalloy. *Addit. Manuf.* **2021**, *48*, 102443. [CrossRef]
60. Gaona-Tiburcio, C.; Aguilar, L.M.R.; Zambrano-Robledo, P.; Estupiñán-López, F.; Cabral-Miramontes, J.A.; Nieves-Mendoza, D.; Castillo-González, E.; Almeraya-Calderón, F. Electrochemical Noise Analysis of Nickel Based Superalloys in Acid Solutions. *Int. J. Electrochem. Sci.* **2014**, *9*, 523–533.
61. Baltazar, M.A.; Bastidas, D.M.; Santiago, G.; Mendoza, J.M.; Gaona, C.; Bastidas, J.M.; Almeraya, F. Effect of silica fume and fly ash admixtures on the corrosion behavior of AISI 304 embedded in concrete exposed in 3.5% NaCl solution. *Materials* **2019**, *12*, 4007. [CrossRef] [PubMed]
62. Buchanan, A.R.; Stansbury, E.E. 4—Electrochemical Corrosion. In *Handbook of Environmental Degradation of Materials*, 2nd ed.; Elsevier: Amsterdam, The Netherlands, 2012; pp. 87–125. [CrossRef]
63. Santiago, G.; Baltazar, M.A.; Galván, R.; López, L.; Zapata, F.; Zambrano, P.; Gaona, C.; Almeraya, F. Electrochemical Evaluation of Reinforcement Concrete Exposed to Soil Type SP Contaminated with Sulphates. *Int. J. Electrochem. Sci.* **2016**, *11*, 4850–4864. [CrossRef]
64. Betova, I.; Bojinov, M.; Laitinen, T.; Mäkelä, K.; Pohjanne, P.; Saario, T. The transpassive dissolution mechanism of highly alloyed stainless steels: I. Experimental results and modelling procedure. *Corros. Sci.* **2002**, *44*, 2675–2697. [CrossRef]
65. Fattah-Alhosseini, A.; Saatchi, A.; Golozar, M.A.; Raeissi, K. The transpassive dissolution mechanism of 316L stainless steel. *Electrochim. Acta* **2009**, *54*, 3645–3650. [CrossRef]
66. Man, C.; Dong, C.; Cui, Z.; Xiao, K.; Yu, Q.; Li, X. A comparative study of primary and secondary passive films formed on AM355 stainless steel in 0.1 M NaOH. *Appl. Surf. Sci.* **2018**, *427*, 763–773. [CrossRef]
67. Bojinov, M.; Betova, I.; Fabricius, G.; Laitinen, T.; Saario, T. The stability of the passive state of iron–chromium alloys in sulphuric acid solution. *Corros. Sci.* **1999**, *41*, 1557–1584. [CrossRef]

68. Núñez-Jaquez, R.E.; Buelna-Rodríguez, J.E.; Barrios-Durstewitz, C.P.; Gaona-Tiburcio, C.; Almeraya-Calderón, F. Corrosion of modified concrete with sugar cane bagasse ash. *Int. J. Corros.* **2012**, *2012*, 451864. [CrossRef]
69. Bojinov, M.; Fabricius, G.; Kinnunen, P.; Laitinen, T.; Mäkelä, K.; Saario, T.; Sundholm, G. The mechanism of transpassive dissolution of Ni–Cr alloys in sulphate solutions. *Electrochim. Acta* **2000**, *45*, 2791–2802. [CrossRef]
70. Huang, J.; Wu, X.; Han, E.H. Electrochemical properties and growth mechanism of passive films on Alloy 690 in high-temperature alkaline environments. *Corros. Sci.* **2010**, *52*, 3444–3452. [CrossRef]
71. Calinski, C.; Strehblow, H.H. ISS depth profiles of the passive layer on Fe/Cr alloys. *J. Electrochem. Soc.* **1989**, *36*, 1328–1331. [CrossRef]
72. Martinez-Villafane, A.; Chacon-Nava, J.G.; Gaona-Tiburcio, C.; Almeraya-Calderon, F.; Dominguez-Patino, G.; Gonzalez-Rodriguez, J.G. Oxidation performance of a Fe–13Cr alloy with additions of rare earth elements. *Mater. Sci. Eng. A* **2003**, *363*, 15–19. [CrossRef]
73. Messinese, E.; Casanova, L.; Paterlini, L.; Capelli, F.; Bolzoni, F.; Ormellese, M.; Brenna, A. A Comprehensive Investigation on the Effects of Surface Finishing on the Resistance of Stainless Steel to Localized Corrosion. *Metals* **2022**, *12*, 1751. [CrossRef]
74. Vodárek, V.; Rožnovská, G.; Kuboň, Z.; Volodarskaja, A.; Palupčíková, R. The Effect of Long-Term Ageing at 475 °C on Microstructure and Properties of a Precipitation Hardening MartensiticStainless Steel. *Metals* **2022**, *12*, 1643. [CrossRef]
75. Ueda, M.; Ikeda, A. Effect of Microstructure and Cr Content in steel on CO_2 Corrosion. In Proceedings of the CORROSION 96, Denver, CO, USA, 24–29 March 1996. Paper No. 96013.
76. Esmaeely, S.N.; Choi, Y.S.; Young, D.; Nesic, S. Effect of calcium on the formation and protectives of iron carbonate layer in CO_2 corrosion. *Corrosion* **2013**, *69*, 912–920. [CrossRef]
77. Keddam, M.; Mattos, O.; Takenouti, H. Mechanism of anodic dissolution of iron-chromium alloys investigated by electrode impedances-II. Elaboration of the reaction model. *Electrochim. Acta* **1986**, *31*, 1159–1165. [CrossRef]
78. Gao, K.W.; Yu, F.; Pang, X.L.; Zhang, G.A.; Qiao, L.J.; Chu, W.Y.; Lu, M.X. Mechanical properties of CO_2 corrosion product scales and their relationship to corrosion rates. *Corros. Sci.* **2008**, *50*, 2796–2803. [CrossRef]
79. Li, J.; Lin, B.; Zheng, H.; Wang, Y.; Zhang, H.; Zhang, Y.; Nie, Z.; Tang, J. Study on pitting corrosion behavior and semi in-situ pitting corrosion growth model of 304 L SS with elastic stress in NaCl corrosion environment. *Corros. Sci.* **2023**, *211*, 110862. [CrossRef]
80. Tranchida, G.; Clesi, M.; Franco, F.D.; Quarto, F.D.; Santamaria, M. Electronic properties and corrosion resistance of passive films on austenitic and duplex stainless steels. *Electrochim. Acta* **2018**, *273*, 412–423. [CrossRef]
81. Ma, L.; Pascalidou, E.M.; Wiame, F.; Zanna, S.; Maurice, V.; Marcus, P. Passivation mechanisms and pre-oxidation effects on model surfaces of FeCrNi austenitic stainless steel. *Corros. Sci.* **2020**, *167*, 108483. [CrossRef]
82. Cabral Miramontes, J.A.; Barceinas Sánchez, J.D.O.; Almeraya Calderón, F.; Martínez Villafañe, A.; Chacón Nava, J.G. Effect of Boron Additions on Sintering and Densification of a Ferritic Stainless Steel. *J. Mater. Eng. Perform.* **2010**, *19*, 880–884. [CrossRef]
83. Gaona-Tiburcio, C.; Montoya, R.M.; Cabral, M.J.A.; Estupiñan, L.F.; Zambrano, R.P.; Orozco, C.R.; Chacon-Nava, J.G.; Baltazar, Z.M.A.; Almeraya-Calderon, F. Corrosion resistance of multilayer coatings deposited by PVD on inconel 718 using electrochemical impedance spectroscopy technique. *Coatings* **2020**, *10*, 521. [CrossRef]
84. Fattah-alhosseini, A.; Taheri Shoja, S.; Heydari Zebardast, B.; Mohamadian Samim, P. An Electrochemical Impedance Spectroscopic Study of the Passive State on AISI 304 Stainless Steel. *Int. J. Electrochem.* **2011**, *2011*, 152143. [CrossRef]
85. Castro, B.E.; Vilche, R.J. Investigation of passive layers on iron and iron-chromium alloys by electrochemical impedance spectroscopy. *Electrochim. Acta* **1993**, *38*, 1567–1572. [CrossRef]
86. Martínez-Villafañe, A.; Almeraya-Calderón, M.F.; Gaona-Tiburcio, C.; Gonzalez-Rodriguez, J.G.; Porcayo-Calderón, J. High-Temperature Degradation and Protection of Ferritic and Austenitic Steels in Steam Generators. *J. Mater. Eng. Perform.* **1998**, *7*, 108–113. [CrossRef]
87. Lv, J.; Liang, T.; Wang, C.; Dong, L. Comparison of corrosion properties of passive films formed on coarse grained and ultrafine grained AISI 2205 duplex stainless steels. *J. Electroanal. Chem.* **2015**, *757*, 263–269.